TABLE I: Silicon Isotope Separation in Flow Systems

	optical geometry	
	parallel	lens (F = 3 m)
transmitted power/W		
vacuum	16.0	16.7
Si_2F_6	9.0	6.7
total pressure/Torr	4.0	4.1
flow rate/mol h^{-1}		
Ar	0.045	0.15
Si_2F_6	0.065	0.20
production rate/mol h^{-1}		
SiF_4	0.0021	0.014
isotope composition/%		
SiF_4		
^{28}Si	59.4	58.0
^{29}Si	5.0	9.0
^{30}Si	35.6	33.0
Si_2F_6[a]		
^{28}Si	92.9	94.7
^{29}Si	4.7	4.4
^{30}Si	2.4	1.0

[a] Unreacted Si_2F_6.

a meaningful extent. The previous studies have shown that SiF_2 does not insert into silicon–hydrogen bonds, although SiH_2 insertions into the bonds are facile reactions.[12,16] We found a considerable amount of polymer deposition on walls in flow systems. Heating of the polymer resulted in evolution of SiF_4, which showed a ^{30}Si content comparable to the SiF_4 produced directly from the IRMPD of Si_2F_6. This fact suggests that the association of SiF_2 is the main channel in the formation of polymer.

The IRMPD of SiF_3Cl, SiF_3Br, and SiF_3CH_3 etc. was also found to give SiF_4 as one of the major products. However, we could not obtain any meaningful selectivity on the formation of $^{29}SiF_4$ or $^{30}SiF_4$.

Flow System. On the basis of the observed results for static systems, we have attempted to separate silicon isotopes from natural Si_2F_6 using a flow technique and a high repetition laser. The laser line was set at P(12), i.e., 951.19 cm^{-1}. The output energy was about 5 J $pulse^{-1}$ and the repetition rate was 10 Hz. However, the energy showed a tendency of decrease with increasing repetition rate. Absorbed energies were determined from differences between the transmitted energies in the presence and absence of Si_2F_6. The fluence of the pulse was estimated to be 0.6–0.7 J cm^{-2} at the front window of the laser. Table I tabulates the experimental parameters and observed results for flow systems.

Si_2F_6 decomposed without foccussing beams. However, the efficiency of decomposition increased by focussing beams slightly using a lens with a 3-m focal length. The optical geometry may compensate a fluence decrease along the beam due to absorption or divergence. We were able to produce silicon at a rate of 0.4 g h^{-1}, where the content of ^{30}Si was 33% and high enough to be used as a tracer in agricultural studies on absorption of silicon by plants. The production rate was found to increase considerably by a sacrifice of an enrichment factor. We also found that the content of ^{28}Si becomes higher than 99.5% or the content of ^{30}Si becomes less than 0.2% in unreacted Si_2F_6 under some conditions. Thus it is possible to produce pure ^{28}Si for crystallographic studies or to produce ^{29}Si-enriched silicon from ^{30}Si-depleted Si_2F_6. The observed enrichment factors seem to be somewhat lower than those estimated from the static results under corresponding conditions. However, the pulse durations are different from each other in the static and flow experiments. A long duration usually reduces an isotope selectivity, because nonresonant molecules excited collisionally undergo multiple photon absorption during the laser pulses.[7] There has been no practical way to separate silicon isotopes except for a magnetic mass separator on a small scale. The present IRMPD method can provide relatively large amounts of silicon isotopes at a low cost.

Registry No. Si_2F_6, 13830-68-7; SiF_4, 7783-61-1; Si_3F_8, 14521-14-3; ^{30}Si, 13981-69-6.

(15) Bowrey, M.; Purnell, J. H. *Proc. R. Soc. London, Ser. A* **1971**, *321*, 341.
(16) Bowery, M.; Purnell, J. H. *J. Am. Chem. Soc.* **1970**, *92*, 2594.

Fluorescence Studies of the Intramolecularly Hydrogen-Bonded Molecules *o*-Hydroxyacetophenone and Salicylamide and Related Molecules

Teruhiko Nishiya,[†] Seigo Yamauchi,[†] Noboru Hirota,*[†] Masaaki Baba,[‡] and Ichiro Hanazaki*[‡]

Department of Chemistry, Faculty of Science, Kyoto University, Kyoto 606, Japan, and Institute for Molecular Science, Okazaki 444, Japan *(Received: April 29, 1986)*

We have investigated the nature of the ground and excited states of intramolecularly hydrogen-bonded *o*-hydroxyacetophenone (OHAP), salicylamide (SAM), methyl salicylate (MS), and 7-hydroxy-1-indanone (7HIN) by means of high-resolution fluorescence spectroscopy. The fluorescence emission and excitation spectra were obtained in durene mixed crystals at 4.2 K and in supersonic helium jets. In the cases of OHAP and SAM, sharp but very weak 0–0 bands were observed both in the emission and excitation spectra followed by the vibronic bands with increased intensities. The vibronic structures are consistent with the tautomerization in the excited state from the keto to the enol form. The potential energy change with respect to the tautomerization reaction coordinate in each molecule is qualitatively explained on the basis of the observed spectra. A particularly drastic change is observed in the case of 7HIN, but we could not obtain any evidence for the presence of the double minimum potential in the excited state.

1. Introduction

Structures and dynamic processes in the excited states of intramolecularly hydrogen-bonded molecules such as methyl salicylate (MS) have attracted much attention in recent years.[3-13] We have investigated fluorescence properties of *o*-hydroxybenzaldehyde (OHBA), *o*-hydroxyacetophenone (OHAP), and 7-

[†] Kyoto University.
[‡] Institute for Molecular Science.

(1) Nagaoka, S.; Hirota, N.; Sumitani, M.; Yoshihara, K. *J. Am. Chem. Soc.* **1983**, *105*, 4220 and references therein.
(2) Nagaoka, S.; Hirota, N.; Sumitani, M.; Yoshihara, K.; Lipczynska-Kochany, E.; Iwamura, H. *J. Am. Chem. Soc.* **1984**, *106*, 6913 and references therein.

0022-3654/86/2090-5730$01.50/0

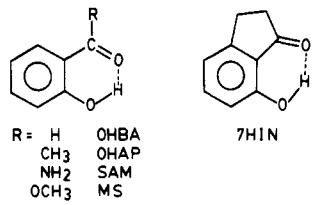

Figure 1. Molecular structures of OHBA, OHAP, SAM, MS, and 7HIN.

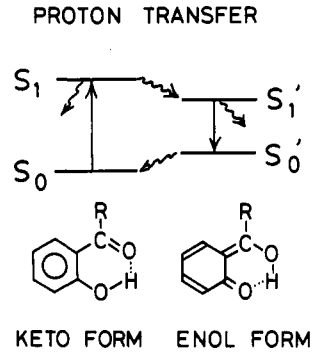

Figure 2. Schematic energy diagram for the dynamic processes of the major species of OHBA and its derivatives.

hydroxy-1-indanone (7HIN) shown in Figure 1 and discussed them in terms of the four-level scheme given in Figure 2.[1,2] This group of molecules is particularly interesting, because they are the simplest among the intramolecularly hydrogen-bonded aromatic molecules. The four-level system would be of great interest in view of the possibilities of making a four-level proton-transfer laser[4] and an information storage device at a molecular level. However, there remain a number of uncertain points about the exact natures of their excited states as well as their spectroscopic properties. For example, it is not certain whether or not a double minimum potential exists along the proton-transfer coordinate. It was suggested that the proton-transferred state is an enol tautomer, but definitive evidence for this assignment is still lacking. Since the absorption and emission spectra taken at room temperature are broad, even the energies of the electronic origins of the excited states are not known accurately except for the case of MS.

In order to understand the dynamic properties of these intramolecularly hydrogen-bonded molecules further, it is thus desirable to have accurate spectroscopic data. In this work, we have attempted to obtain high-resolution fluorescence excitation and emission spectra of OHBA, OHAP, MS, salicylamide (SAM), and 7HIN. Though the high-resolution fluorescence spectra of MS have been studied in supersonic free jets[6,7] and in solid matrices,[5] others have not been studied in detail. It was thought that a systematic study of the fluorescence spectra of this group would be helpful in understanding their dynamic properties as well as the natures of their excited states. Here we have found that the fluorescence spectra are rather sensitive to the nature of the group attached to the carbonyl group. Since the O–H···O length in 7HIN is expected to be longer than those in others, comparison of 7HIN with others should reveal the effect of elongation of the O–H···O length on their spectroscopic properties. This comparison would be interesting in view of the difference found for the dynamic properties between 7HIN and others.[2,14]

To obtain high-resolution spectra, we have employed two different techniques: low-temperature spectroscopy using mixed crystals and supersonic jet spectroscopy. The usefulness of the former technique is well established, but it has not been utilized much in studying the proton-transfer problem. Here we obtained spectra at 4.2 K by using durene mixed crystals. The supersonic jet spectroscopy is expected to give highly resolved fluorescence emission and excitation spectra by eliminating complications due to thermal and solvent effects. Indeed it has provided useful information in the case of MS.[6,7] Here we discuss the natures of the ground and excited states of these molecules on the basis of the obtained spectra.

2. Experimental Section

A. Sample Preparation. Commercially obtained OHBA, OHAP, and MS were purified by repeated vacuum distillation and by column chromatography on Kiesel gel G (Merck). SAM was recrystallized twice from chloroform. 7HIN is a gift from Prof. H. Iwamura of the Institute for Molecular Science, which was synthesized and purified according to the method described elsewhere.[2] Durene was chromatographed over an activated alumina column, recrystallized twice from ethanol, and zone refined extensively. Durene crystals containing small amounts of guest molecules were grown from melts by the standard Bridgman method.

B. Absorption and Emission Spectroscopy. Absorption spectra were taken with a Shimadzu UV-200 double-beam spectrometer. Fluorescence emission and excitation spectra were taken with a Spex Fluorolog fluorescence spectrometer.

C. Fluorescence Spectroscopy in Supersonic Free Jets. A pulsed supersonic nozzle beam setup is described elsewhere.[15] We employed the second harmonics of the output from the YAG laser-pumped dye laser (Quantel, bandwidth 0.1 cm^{-1}, pulse duration 15 ns, pulse energy 1 mJ) as the excitation light source. The laser was operated synchronously with the supersonic nozzle at 5 Hz. The sample was reserved in a stainless steel reservoir through which argon was flowed. This sample source and the nozzle were heated in order to get sufficient vapor pressure.

D. Fluorescence Spectroscopy in Low-Temperature Single Crystals. The sample was immersed into a Pyrex liquid-helium double Dewar with quartz windows or set in a continuous-flow liquid-helium cryostat (Oxford, CF-204). The fluorescence emission passed through a glass filter was analyzed by a monochromator (Spex 1704) and detected by a photomultiplier (Hamamatsu, R-928 and R-1104). Signal processing of the photomultiplier output was achieved with a boxcar integrator (PAR, Model 162). The excitation light source was an excimer laser (Lumonics, TE-861M; XeCl, 308 nm) for the measurement of the emission spectra and a YAG laser-pumped dye laser for the excitation spectra.

3. Results

A. Fluorescence Emission and Excitation Spectra in Durene Mixed Crystals at 4.2 K. We have obtained the fluorescence emission and excitation spectra of OHAP, SAM, MS, and 7HIN in the durene mixed crystals. However, photoinduced isomerization discussed previously[1] and formation of duryl radical prevented us from obtaining the OHBA spectrum without contamination, though the general feature of the spectrum appears to be similar to that of OHAP. In the remaining molecules both fluorescence emission and excitation spectra consist of two regions: in the emission spectra very weak short-wavelength regions and strong longer wavelength regions, and in the excitation spectra vice versa. In the following sections, we will describe each case.

a. Emission Spectra. The fluorescence emission spectra of OHAP, SAM, and MS in the durene mixed crystals obtained at

(3) Brackmann, U.; Ernsting, N. P.; Ouw, D.; Schmitt, K. *Chem. Phys. Lett.* **1984**, *110*, 319.
(4) Chou, P.; McMorrow, D.; Aartsma, T. J.; Kasha, M. *J. Phys. Chem.* **1984**, *88*, 4596.
(5) Goodman, J.; Brus, L. E. *J. Am. Chem. Soc.* **1978**, *100*, 7472.
(6) Felker, P. M.; Lambert, W. R.; Zewail, A. H. *J. Chem. Phys.* **1982**, *77*, 1603.
(7) Heimbrook, L.; Kenny, J. E.; Kohler, B. E.; Scott, G. W. *J. Phys. Chem.* **1983**, *87*, 280.
(8) Kuper, J. W.; Perry, D. S. *J. Chem. Phys.* **1984**, *80*, 4640.
(9) Mordzinsky, A.; Grabowska, A.; Teuchner, K. *Chem. Phys. Lett.* **1984**, *111*, 383.
(10) Van Benthem, M. H.; Gillispie, G. D. *J. Phys. Chem.* **1984**, *88*, 2954.
(11) Bondybey, V. E.; Haddon, R. C.; English, J. H. *J. Chem. Phys.* **1984**, *80*, 5432.
(12) Rentzepis, P. M.; Bondybey, V. E. *J. Chem. Phys.* **1984**, *80*, 4727.
(13) Smulevich, G. *J. Chem. Phys.* **1985**, *82*, 14.
(14) Nishiya, T.; Hirota, N.; Fujiwara, Y.; Itoh, M. *J. Am. Chem. Soc.* **1986**, *108*, 3880.
(15) Baba, M.; Hanazaki, I. *Chem. Phys. Lett.* **1983**, *103*, 93.

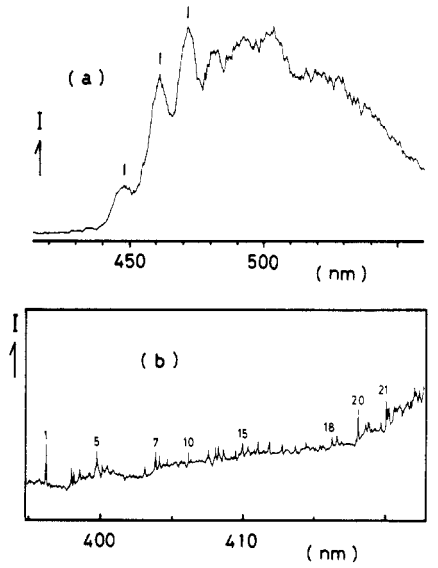

Figure 3. Fluorescence spectra of OHAP in a durene mixed crystal at 4.2 K obtained by exciting at 308 nm. (Intensity (I) is given in arbitrary units.) (a) Long-wavelength region; (b) short-wavelength region.

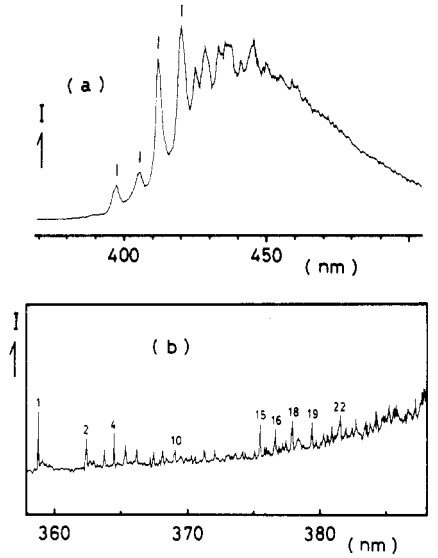

Figure 4. Fluorescence spectra of SAM in a durene mixed crystal at 4.2 K obtained by exciting at 308 nm. (Intensity (I) is given in arbitrary units.) (a) Long-wavelength region; (b) short-wavelength region.

4.2 K by excimer laser (308-nm) excitation are shown in Figure 3-5. The long-wavelength regions of the fluorescence spectra of OHAP and SAM shown in Figures 3a and 4a, respectively, have much higher intensities than the short-wavelength regions. Partially resolved vibronic structures are observed in this region. The short-wavelength regions shown in Figures 3b and 4b reveal highly resolved structures, full width at half maximum (fwhm) of each band being 4–10 cm^{-1}. A sequence of sharp vibronic lines including several progressions are built on the origin at 25237 cm^{-1} (396.1 nm) for OHAP and at 27864 cm^{-1} (358.8 nm) for SAM. The spectra become virtually a continuum at 2000–2500 cm^{-1} below the origins. The Franck–Condon maxima of the emissions are located at 20 000 cm^{-1} (500 nm) for OHAP and 22 700 cm^{-1} (440 nm) for SAM. In the case of MS, the relative intensity of the short-wavelength region is much higher as seen in Figure 5. The general appearance of the spectrum is similar to those of the spectra in supersonic jets and in a neon matrix reported in the literature.[5-8] The 0–0 band is observed at 29 162 cm^{-1} (342.8 nm), and the Franck–Condon maximum is located at 22 700 cm^{-1} (440 nm). The short wavelength region of the 7HIN spectrum is too weak to reveal the origin band. The emission intensity increases abruptly at about 20 800 cm^{-1} (480 nm), with the Franck–Condon maximum at 18 900 cm^{-1} (530 nm) as seen in Figure 9.

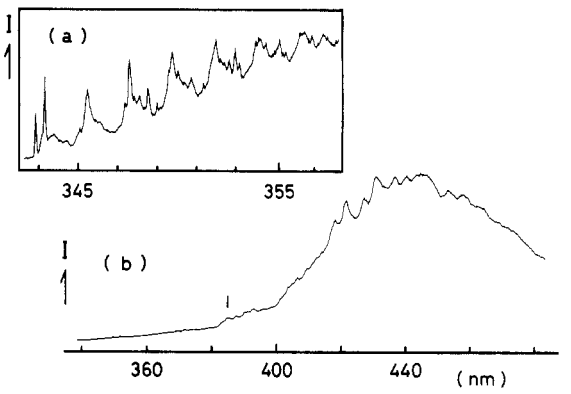

Figure 5. Fluorescence spectra of MS in a durene mixed crystal at 4.2 K obtained by excitation at 308 nm. (Intensity (I) is given in arbitrary units.) (a) Short-wavelength region; (b) overview.

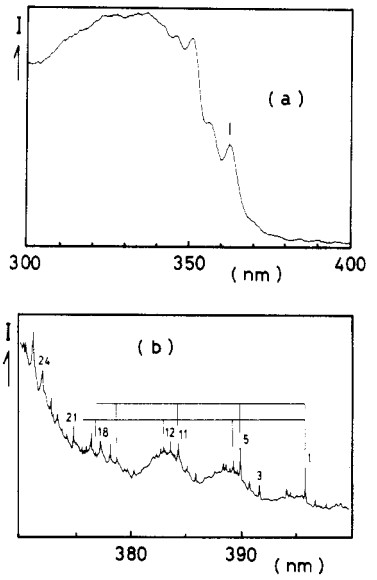

Figure 6. Fluorescence excitation spectra of OHAP in a durene mixed crystal at 4.2 K obtained by monitoring at the long-wavelength fluorescence region. (Intensity (I) is given in arbitrary units.) (a) Overview; (b) region near 0–0 transition.

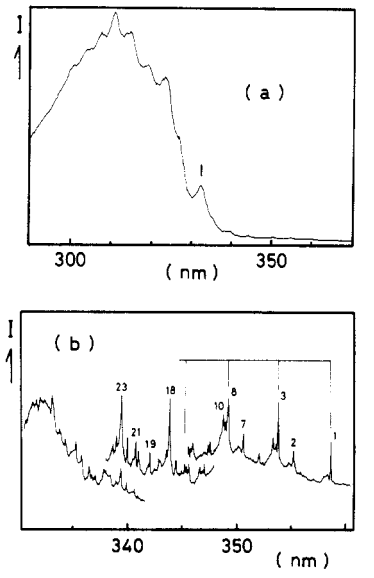

Figure 7. Fluorescence excitation spectra of SAM in a durene mixed crystal at 4.2 K obtained by monitoring at the long-wavelength fluorescence region. (Intensity (I) is given in arbitrary units.) (a) Overview; (b) region near 0–0 transition.

b. Excitation Spectra. The excitation spectra monitored in the long-wavelength regions of the fluorescence of OHAP and

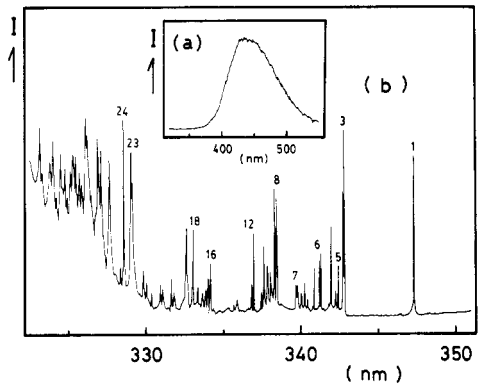

Figure 8. (a) Fluorescence emission spectrum of SAM in a supersonic helium jet obtained by 308-nm excitation. (b) Fluorescence excitation spectrum of total fluorescence emission of SAM in a supersonic helium jet. (Intensity (I) is given in arbitrary units.)

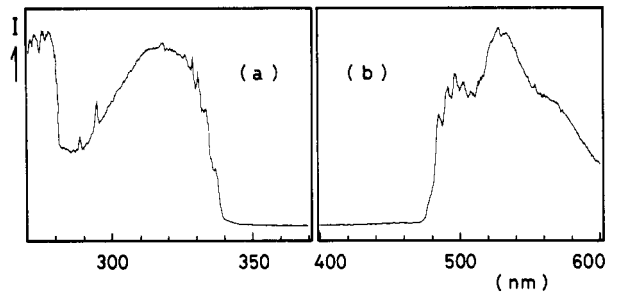

Figure 9. Fluorescence (a) excitation and (b) emission spectra of 7HIN in a durene mixed crystal at 4.2 K. Exciting and monitoring wavelengths were 320 and 520 nm. (Intensity (I) is given in arbitrary units.)

SAM in the durene mixed crystals at 4.2 K are shown in Figures 6 and 7. Owing to extremely low emission intensities in the short-wavelength regions, we were only able to measure their excitation spectra by monitoring the long wavelength regions. The spectra show a sequence of sharp vibronic lines (fwhm = 6–10 cm^{-1}) in the long-wavelength regions, including several progressions built on the origins at 25 254 cm^{-1} (395.9 nm) for OHAP and at 27 871 cm^{-1} (358.7 nm) for SAM and become quite congested at 1500–1700 cm^{-1} above the origins. The positions of the 0–0 bands are in good agreement with those of the corresponding emission bands within experimental error. The coincidence of the 0–0 bands in the absorption and emission implies that the laser can directly excite the vibrationless state of the tautomer. In the short wavelength regions, partially resolved structures are observed. The Franck–Condon maxima of the excitation spectra are located at 29 800 cm^{-1} (335 nm) for OHAP and at 32 300 cm^{-1} (310 nm) for SAM. The long-wavelength region of the excitation spectrum of 7HIN is also extremely weak, and the 0–0 band of the absorption could not be detected. The excitation spectrum shows the Franck–Condon maximum at 31 300 cm^{-1} (320 nm).

B. Fluorescence Emission and Excitation Spectra in Supersonic Helium Jets. We have examined both emission and excitation spectra of OHBA, OHAP, SAM, and MS in supersonic helium jets. We obtained well-resolved excitation spectra in SAM and MS, but we failed to observe well-resolved excitation spectra in the cases of OHBA and OHAP, though we have tried experiments at different sample temperatures and stagnation pressures.

a. Emission Spectra. The fluorescence emission spectrum of SAM excited at 308 nm (in the vicinity of the Franck–Condon maximum in the SAM absorption) in a supersonic helium jet is shown in Figure 8a. Similar structureless emission spectra were obtained on excitation at the different wavelengths, particularly at the sharp vibronic bands in the excitation spectra including the 0–0 band and also in the case of other molecules.

b. Excitation Spectra. The excitation spectrum of MS is similar to that reported by Heimbrook et al.,[7] though the relative peak intensities are somewhat different. The excitation spectrum of the long-wavelength region of the fluorescence of SAM in a supersonic helium jet is shown in Figure 8b. The spectrum shows

TABLE I: Vibrational Analysis of the Fluorescence Emission Spectra of OHAP and SAM in the Durene Mixed Crystals at 4.2 K

no.	ν/cm^{-1}	OHAP assignment	ν/cm^{-1}	SAM assignment
1	0	origin (25 237 cm^{-1})	0	origin (27 864 cm^{-1})
2	112	C—COR torsion?	280	C—OH bending?
3	125	C—OH torsion?	381	C—COR bending?
4	151	?	435	CCC bending
5	225	2 × 112, C–OH bending?	499	C=O bending
6	434	CCC bending	565	CCC bending
7	480	C=O bending	639	CCC bending
8	499	?	660	280 + 381
9	532	?	710	CCC bending
10	621	CCC bending	776	280 + 449
11	706	CCC bending	936	435 + 499
12	736	112 + 621	944	381 + 565
13	749	125 + 621	996	435 + 565, 2 × 499
14	771	151 + 621	1215	?
15	849	2 × 112 + 621	1240	C—OH stretching
16	916	434 + 480	1323	O—H bending
17	960	2 × 480	1377	?
18	1221	C—OH stretching	1410	C—R stretching
19	1242	2 × 621	1515	280 + 1240
20	1326	O–H bending	1578	C—C stretching
21	1440	3 × 621, 112 + 1326	1595	C—C stretching
22	1451	125 + 1326	1662	C=O stretching

a sequence of sharp vibronic lines (fwhm = 4–8 cm^{-1}), including several progressions built on the origin at 28 788 cm^{-1} (347.3 nm). The origin band of the gas-phase spectrum shifts by 870 cm^{-1} to the blue from that of the condensed-phase spectrum. A similar shift has also been observed in the case of MS.[6,7] The shift on going from the gas to the condensed phase is due to host stabilization of the guest excited state relative to the ground state in the condensed phase. Prominent bands observed in the condensed-phase spectrum are also observed in the gas-phase spectrum. The gas-phase spectrum is free from contamination by the phonon sidebands and inhomogeneous broadening, but the vibrational structure in the gas-phase spectrum is more complicated than in the condensed-phase spectrum with activities of several additional low-frequency modes. Another notable observation is the higher relative intensities of the bands in the low-energy region, which was previously noted by Heimbrook et al. in the case of MS.[7]

C. Vibronic Assignments. A complete listing of the observed bands and a set of vibrational assignments of the emission and excitation spectra are given in Tables I and II, respectively, for OHAP and SAM in the condensed and gas phases. The observed emission and excitation spectra can be assigned with combinations and overtones of about 10 fundamentals. Each fundamental mode in the emission spectra was assigned on the basis of the infrared and Raman spectral data[16-24] of benzaldehyde,[16] acetophenone,[17-21] benzamide,[17,18] and OHAP[24] and are given in Table I.

4. Discussion

A. Fluorescence Spectra and the Vibrational Modes in the Ground States. The 0–0 bands of the fluorescence of all the molecules studied here are very weak, showing that the fluorescent states have structures quite different from those of the ground states. The fluorescence spectra of OHAP and SAM seen in Figures 3a and 4a, respectively, show partially resolved vibronic

(16) Zwarich, R.; Smolarek, J.; Goodman, L. *J. Mol. Spectrosc.* **1971**, *38*, 336.
(17) Green, J. H. S.; Harrison, D. J. *Spectrochim. Acta Part A* **1977**, *33A*, 583.
(18) Weckherlin, V. S.; Luttke, W. Z. *Elektrochem.* **1960**, *64*, 1228.
(19) Gambi, A.; Giorganni, S.; Passerini, A.; Visinoni, R.; Ghersetti, S. *Spectrochim. Acta, Part A* **1980**, *36A*, 871.
(20) Silver, H. G.; Wood, J. L. *Trans. Faraday Soc.* **1964**, *60*, 5.
(21) Campajnaro, G. E.; Wood, J. L. *J. Mol. Struct.* **1970**, *6*, 117.
(22) Nyquist, R. A. *Spectrochim. Acta, Part A* **1963**, *19A*, 1655.
(23) Green, J. H. S.; Harrison, D. J.; Kynaston, W. *Spectrochim. Acta, Part A* **1971**, *27A*, 2199.
(24) Gupta, V. P.; Gupta, D.; Jain, S. M. *Ind. J. Pure Appl. Phys.* **1976**, *14*, 846.

TABLE II: Vibrational Analysis of the Fluorescence Excitation Spectra of OHAP and SAM in the Durene Mixed Crystals at 4.2 K and in Supersonic Helium Jets

	OHAP		SAM		
no.	durene ν/cm^{-1}	assignment[a]	durene ν/cm^{-1}	He jet ν/cm^{-1}	assignment
1	0	origin (25 254 cm^{-1})	0		origin (27 871 cm^{-1})
				0	origin (28 788 cm^{-1})
2	109	ν_1	265		ν_1
3	269	ν_2	377	376	ν_2
4	329	ν_3	391		ν_3
5	381	ν_4	415	411	ν_4
6	423	ν_5	517	515	ν_5
7	469	?	634	647	ν_6
8	484	$\nu_1 + \nu_4$	750	753	$2\nu_2$
9	649	$\nu_2 + \nu_4$	771		$\nu_2 + \nu_3$
10	703	ν_6	788	787	$\nu_2 + \nu_4$
11	753	$2\nu_4$	856		ν_7
12	801	ν_7	889	894	$\nu_2 + \nu_5$
13	844	$2\nu_5$	902		$\nu_1 + \nu_6$
14	863	$2\nu_2 + \nu_3$	1018		$\nu_1 + 2\nu_2$
15	1030	$\nu_2 + 2\nu_4$	1051		$\nu_4 + \nu_6$
16	1137	$3\nu_4$	1123	1130	$3\nu_2$
17	1180	$\nu_4 + \nu_7$	1190	1195	?
18	1241	ν_8	1235	1231	ν_9, $\nu_2 + \nu_7$
19	1269	$3\nu_5$	1381		ν_{10}
20	1300	ν_9	1472		ν_{11}
21	1414	ν_{10}	1495	1505	$4\nu_2$
22	1516	ν_{11}	1560	1545	ν_{12}
23	1559	$2\nu_4 + \nu_7$	1608	1596	ν_{13}
24	1617	ν_{12}	1649	1639	$\nu_4 + \nu_9$
25	1682	$\nu_3 + \nu_{10}$	1678		?

[a] The numbering of the mode does not correspond to the normal mode.

structures. In the case of OHAP, the three bands indicated by vertical lines are located at 3000, 3500, and 4050 cm^{-1} below the origin and are quite broad (fwhm = 400–500 cm^{-1}). Previously observed infrared absorption spectra of OHAP revealed that the hydroxy O–H stretching vibration produces a very broad absorption band extending over the range 2500–3500 cm^{-1}, with the maximum near 3050 cm^{-1}.[22-24] The position of the first band seen in Figure 3a coincides with this frequency. We therefore assign this band as the O–H stretching vibration. The same assignment is also possible in the case of SAM seen in Figure 4a. It was noted in the jet spectrum of MS that the 3220-cm^{-1} vibration is active and this mode was assigned to the O–H stretching vibration.[6] This mode is also prominent in the durene crystal and indicated by a vertical line in Figure 5b.

The fluorescence spectra of OHAP and SAM seen in Figures 3b and 4b show several vibrational modes associated with the carbonyl and hydroxy groups. For example, 480 (499), 1221 (1240), and 1326 (1323) cm^{-1} modes of OHAP (SAM) are assigned to the carbonyl C=O bending, ring carbon–hydroxy oxygen C–OH stretching, and hydroxy O–H bending vibrations, respectively. The 1662-cm^{-1} band of SAM may be assigned to the carbonyl C=O stretching band, but this band was not clearly identified in the spectrum of OHAP because of the spectral congestion in this region. A progression with 500-cm^{-1} intervals built on the band 3000 cm^{-1} (2700 cm^{-1}) below the origin is observed for OHAP (SAM) in Figure 3a (Figure 4a), which is ascribed to the C=O bending vibration. Other low-frequency modes of OHAP and SAM are assigned to the torsions and bending vibrations as shown in Table I. Another notable observation is that the vibrational structure of the short-wavelength region is very different depending on the molecules, as seen in Figures 3–5. In particular, the 180-cm^{-1} progression prominent in the MS spectrum does not show up in the other spectra. It was previously suggested that this mode is associated with an out-of-plane bending motion of the "ring" that includes the intramolecular hydrogen bond.[6] However, if this is the case, this mode should appear in the other molecules. The 180-cm^{-1} mode may be due to the internal rotation of the methyl group.

Summarizing the main vibrational structures of the spectra, we can conclude that the vibrational bands related to the proton motion and their overtones and combination bands are prominent. This feature is consistent with the generally conceived view that proton transfer takes place in the excited states. Furthermore, the vibrations associated with the skeletal motions are also active, indicating that the entire molecular geometry is changed in the excited-state tautomerization.

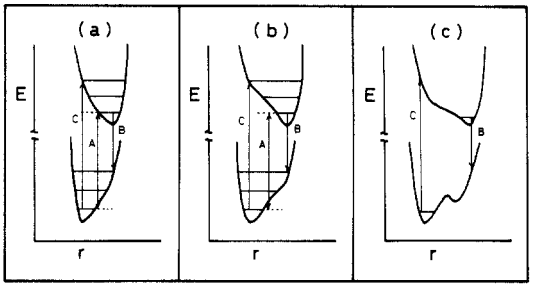

Figure 10. Schematic potential energy curves for the tautomerization in the ground and excited states. (Energy (E) is given in arbitrary units. r represents the reaction coordinate.) (a) MS; (b) OHAP and SAM; (c) 7HIN.

TABLE III: Transition Energies (A, B, and C) and Stokes Shifts ($C - B$) of OHAP, SAM, MS, and 7HIN in the Durene Mixed Crystals at 4.2 K[a,b]

	A, cm^{-1}	B, cm^{-1}	C, cm^{-1}	$C - B$, cm^{-1}
OHAP	25 237	20 000	29 800	10 300
	25 254			
SAM	27 864	22 700	32 300	9 600
	27 871			
MS	29 162	22 700	32 300	9 600
7HIN		18 900	31 300	12 400

[a] See Figure 10. Values of B and C are estimated from the positions of the corresponding Franck–Condon maxima.

B. Franck–Condon Envelope and the Nature of the Emitting State. In the process of tautomerization, the molecule changes the geometry along the coordinates which are associated with the vibrations discussed in the previous section. To be exact, one has to discuss the potential energy surfaces in the multidimensional space. For the sake of simplicity, however, we will discuss here the potential changes of the ground and excited states using simple schematic potential curves along the reaction coordinate.

The emission and excitation spectra of MS in durene are explained by the distorted potential curves shown in Figure 10a. The 0–0 band observed at 342.8 nm corresponds to the transition indicated by the vertical line A (29 162 cm^{-1}). The Franck–Condon maxima of the emission and excitation spectra correspond to lines B (22 700 cm^{-1}) and C (32 300 cm^{-1}), i.e., 6500 cm^{-1} below and 3100 cm^{-1} above the origin, respectively.

In the case of OHAP (SAM) in durene, the origin is also considered to be common for the emission and excitation spectra within experimental error, being 25 237 (27 864) and 25 254 (27 871) cm^{-1}, respectively. The intensity of the 0–0 band is much weaker than in MS and rises abruptly at about 3000 (2700) cm^{-1} below the origin in the emission spectrum. Similarly, it rises at about 2300 (2200) cm^{-1} above the origin in the excitation spectrum. The Franck–Condon maxima of the emission and excitation spectra are 5200 (5200) cm^{-1} below and 4600 (4400) cm^{-1} above the origin, respectively. The intensities of the Franck–Condon maxima of the emission spectra are more than 100 times as strong as those of the origins. It suggests larger distortions of the potential in both OHAP and SAM than in MS, and the spectra are qualitatively explained by the potential curve shown in Figure 10b. The energies for transitions A, B, and C are given in Table III. The positions of the Franck–Condon maxima in the fluorescence emission and excitation spectra are close to the second harmonics of the O–H stretching vibrations, and those of the abrupt intensity rises in the spectra correspond to the fundamentals of these vibrations, as shown in Figure 10.

Two observations seem to be particularly noteworthy. The first one is that the potential curves are rather sensitive to the nature of the group attached to the carbonyl group despite the similarity

of the molecular structure. The second one is that the relative stability of the excited singlet state changes considerably in the order of OHAP (25 237 cm^{-1}), SAM (27 864 cm^{-1}), and MS (29 162 cm^{-1}). The effect of the attached group on the electron density on the oxygen atom may be large enough to cause the change in the position and the energy of the potential minimum for the structural change.

In the case of 7HIN, the 0–0 bands of the emission and excitation spectra have not been detected, and both spectra show very abrupt increases of the intensities. This observation indicates that the potential curves are much more distorted along the reaction coordinate and may be explained in the following way. Since the O–H···O distance is significantly longer in this molecule, the displacement of the proton in the process of proton transfer is expected to be much larger than in the other molecules, causing a larger change in the potential energy. The observed spectrum is explained by the potential curve shown in Figure 10c. The result of our recent two-step laser excitation (TSLE) fluorescence measurements suggests the presence of a shallow double minimum potential in the ground state.[14] However, in the present work we could not detect any evidence for the existence of a double minimum potential for the excited state.

C. Vibrational Modes and the Structures in the Excited State. The distortion of the excited-state potential surface with respect to that of the ground state makes vibrational assignment of the excitation spectra extremely difficult. The infrared spectral data of the ground states are no longer useful.

However, the observed vibrational structures are consistent with the keto–enol tautomerization associated with the proton transfer. We first note that the modes coupled to the proton transfer are active in the excitation spectra. For example, the peak located at 1241 cm^{-1} (1235 cm^{-1}) above the origin of the spectrum of OHAP (SAM) in Figure 5b (Figure 6b) may be assigned to the stretching vibration of the C–OH group which corresponds to the carbonyl C=O in the ground state. On the other hand, the peak at 1617 cm^{-1} (1608 cm^{-1}) can be assigned to the ring carbon–oxygen stretching vibration which has a considerable double-bond character in the excited state. The first broad band indicated by a vertical line in the OHAP (SAM) excitation spectrum in Figure 5a (Figure 6a) is located at 2300 cm^{-1} (2200 cm^{-1}) above the origin. This mode is considered to be associated with the O–H stretching vibration as in the case of the emission spectra. We also note that other low-frequency modes are very active in the excitation spectra. In particular, a progression of the 381-cm^{-1} (377-cm^{-1}) vibration of OHAP (SAM) is very remarkable. It was previously noted that the 347-cm^{-1} vibration is very active in the excitation spectrum of MS, and this was assigned to the ν_{6a} ring bending vibration.[7] A similar assignment can be made to these vibrations. Other modes associated with the skeletal vibrations appear to be active, making the excitation spectra rather complex, particularly in the jet spectrum of SAM. These activities suggest distortions of the excited-state potential surfaces along the coordinates of the skeletal motions which are consistent with the assignment of the fluorescent-state structure to the enol tautomer.

D. Comment on the Jet Spectra. The most notable characteristics of the excitation spectra obtained in the free jets compared with the condensed-phase spectra are the high relative intensities of the 0–0 and low-frequency bands with respect to the Franck–Condon maximum. This was noted previously by Heimbrook et al.[7] for MS, and we have also confirmed their result. In the case of SAM, the relative intensities of the low-frequency bands are not so high as in MS, but they are still higher than those of the condensed-phase spectrum. This is presumably due to the low quantum yields for higher vibrational levels in the excited singlet states of the isolated molecules caused by the increased rate of nonradiative decay for these levels. In the solid matrices, the vibrational relaxation within the electronically excited state could compete with the nonradiative decay. This new channel, which is not effective in the isolated molecules, brings the molecule down to the lower vibrational levels in the excited state, where the nonradiative decay is very slow. The quantum yield for the excitation spectrum at higher vibrational levels would thus be enhanced in the condensed phase. The jet excitation spectrum is observed even 3300 cm^{-1} above the origin. This feature is different from the case of MS in which the intensity is quickly weaken at 1200 cm^{-1} above the origin.[7,8] The quantum yield of fluorescence probably decreases more slowly for SAM on increasing excess energy.

In the case of SAM, almost all the vibrational bands seen in the condensed-phase excitation spectrum were also observed in the jet excitation spectrum. A continuum appears in the jet excitation spectrum about 1800 cm^{-1} above the origin which may be attributed to the coupling with another electronic state. Similar continuum is also observed in the condensed-phase excitation spectrum. The exact reason for the failure in observing well-resolved jet spectra of OHBA and OHAP is not known, though the quantum yields of fluorescence of these molecules are low. Further investigations are needed to clarify these points.

5. Summary and Conclusion

We have studied the high-resolution fluorescence emission and excitation spectra of OHAP, SAM, MS, and 7HIN in the durene mixed crystals and in the supersonic helium jets. The high-resolution spectra reveal vibronic structures which are consistent with the tautomerization in the excited states from the keto to the enol forms. The change in the potential energy surface associated with the tautomerization, however, differs significantly depending on the individual molecule despite the similarity of the molecular structure. The change in the potential energy in each case is qualitatively explained on the basis of the obtained spectra. A particularly drastic change was observed in the case of 7HIN in which the O–H···O distance is expected to be larger. No evidence for the presence of the double minimum potential was detected for the excited states of their molecules.

Acknowledgment. We are grateful to Prof. H. Iwamura of the Institute for Molecular Science for the generous gift of 7HIN and are greatly indebted to Dr. K. Hayasaka of the Low Temperature Center of the Institute for supplying us liquid helium.

This research was supported by a Grant-In-Aid from the Mitsubishi Foundation.

Registry No. OHAP, 118-93-4; SAM, 65-45-2; MS, 119-36-8; 7HIN, 6968-35-0.